Dalton Transactions

Accepted Manuscript



This is an *Accepted Manuscript*, which has been through the Royal Society of Chemistry peer review process and has been accepted for publication.

Accepted Manuscripts are published online shortly after acceptance, before technical editing, formatting and proof reading. Using this free service, authors can make their results available to the community, in citable form, before we publish the edited article. We will replace this Accepted Manuscript with the edited and formatted Advance Article as soon as it is available.

You can find more information about *Accepted Manuscripts* in the **Information for Authors**.

Please note that technical editing may introduce minor changes to the text and/or graphics, which may alter content. The journal's standard <u>Terms & Conditions</u> and the <u>Ethical guidelines</u> still apply. In no event shall the Royal Society of Chemistry be held responsible for any errors or omissions in this *Accepted Manuscript* or any consequences arising from the use of any information it contains.



Selective oxidation of cyclohexane on a novel catalyst Mg-Cu/SBA-15 by molecular oxygen

Xiaogang Duan,^a Weimin Liu,^a Lumin Yue,^a Wei Fu,^a Minh Ngoc Ha,^b Jun Li,*^a,
Guanzhong Lu.^{a, b}

- [a] Research Institute of Applied Catalysis, School of Chemical and Environmental Engineering, Shanghai Institute of Technology, Shanghai 201418, P. R. China. E-mail: Junliecust0967@sina.com
- [b] Key Laboratory for Advanced Materials, Research Institute of Industrial Catalysis, East China University of Science and Technology, Shanghai 200237, PR China

Abstract: novel catalysts *x*Mg-2.3Cu/SBA-15 with copper and magnesium oxide co-supported on mesoporous silica were synthesized by an impregnation method. The newly synthesized catalysts were characterized by a series of techniques such as BET, XRD, H₂-TPR, UV-vis, XPS, EDS and TEM. The catalytic performance was evaluated by using selective oxidation of cyclohexane with molecular oxygen as the oxidant in a solvent free system. The incorporation of magnesium improved the dispersion of copper oxide and prevented the deep oxidation of cyclohexanol and cyclohexanone. The selectivity of K/A oil was up to 99.3% with 12% conversion of cyclohexane over catalyst 1.2Mg-2.3Cu/SBA-15. To our knowledge, this is the best result for the heterogeneous oxidation of cyclohexane by O₂.

Introduction

The oxidation of cyclohexane to cyclohexanol and cyclohexanone (K/A oil),

which are intermediates in the production of adipic acid and caprolactam, is of great importance in the processes to manufacture nylon-6 and nylon-66 polymers. 1-3 However, cyclohexane oxidation is considered to be the least efficient in major industrial chemical processes, 1-3 the conversion of the matrix is usually lower than 5% in order to obtain high selectivity of cyclohexanone and cyclohexanol since the target products are more active than the reactant. On the other hand, the deteriorating environmental pressure urges people to search for more efficient catalytic systems.

Molecular oxygen is thought to be the most clean and readily available oxidant. Recent years, great efforts have been devoted to explore catalysts and heterogeneous catalytic system with dioxygen as the oxidant for the selective oxidation of cyclohexane, some promising reaction system were reported. In addition to molecular oxygen, Other oxidants, such as tert-butyl hydroperoxide or hydrogen peroxide, were also investigated with solid-state catalysts, titanium silicalite-2 (TS-2), or metal-incorporated mesoporous molecular sieves, and microporous aluminosilicate molecular sieves and microporous molecular sieves, which may result in contamination of products and environmental problems. There is a long way from achieving high yields in industrial scale by the heterogeneous reaction system with molecular oxygen as oxidant. Developing novel catalysts may be crucial for the system with O₂ as the oxidant.

Transition-metal-supported catalysts attracted great attention of researchers for the activation of molecular oxygen. Published results indicated the catalytic performance of the catalysts largely depended on the dispersion of the active components, ^{5, 6, 11} which may be subject to the supporter. Mesoporous silica materials, such as SBA-15 with ordered and controllable porous structure, high surface area, excellent mechanical properties, pore volume and thermal stability, are often used as suitable catalyst supporters to facilitate the access of the substrates to the active sites and provide high dispersion of the active components.¹²

Transition metals, owing to their specific electronic structures, were heavily reported as efficient components. 1-5, 11 Gold nanoparticles (Au NPs) supported on mesoporous silica have been found to display a high catalytic activity in oxidation reaction. 13-16 As it is well known that the catalytic properties of gold nanoparticles are closely related to their morphology and particle size. 17,18 However, Au NPs are unstable and liable to aggregation. Besides, the morphology and particle size of Au NPs are unstabilized and not easily controlled on support surface by traditional methods. Thus, other metals have also been taken into consideration. Copper, locating at the same elemental group as Au, have been used in many heterogeneous redox reactions including selective oxidation of cyclohexane, and some interesting results were obtained. 6,19-21 However, the copper species catalysts exhibited ~9% conversion of cyclohexane and ~80% selectivity of K/A oil. The higher conversion of cyclohexane and better selectivity of K/A oil are desired.

Recent years, chemists disclosed that the incorporation of Mg into silica led to a very better catalytic performance and stability of catalyst. 22-25 Yoshida H and co-workers 22 reported that silica-supported magnesium catalyst could promote the

oxidation of propene to propylene oxide by O₂ under illumination. Vizcaíno A J et al.²⁴ revealed that Mg enhanced the catalytic performance of CuNi/SBA-15 catalysts on ethanol steam reforming, giving higher hydrogen selectivity and lower coke deposition. In addition, Knochel P et al.²⁵ reported the sluggish reactivity of organozinc reagents towards aldehydes and ketones can be dramatically improved by the addition of MgCl₂. In conclusions, the above mentions spur us to think over the intrinsically synergetic effects of magnesium species. With a question whether the magnesium species would have effects on the selectivity of K/A oil in cyclohexane oxidation in mind, we designed and fabricated a few novel catalysts by co-supporting copper and magnesium oxide on mesoporous silica and studied their catalytic performance.

In this work, the catalysts xMg-2.3Cu/SBA-15 were prepared by impregnation method. The catalytic effects of xMg-2.3Cu/SBA-15 were examined for the oxidation of cyclohexane with molecular oxygen as oxidant. The bi-component catalysts exhibited a special catalytic activity and selectivity of K/A oil in the liquid phase oxidation of cyclohexane.

Results and Discussion

Figure 1

Figure 2

Figure 3

The low-angle powder XRD spectra of all samples are showed in Figure 1, a

sharp main diffraction peak and two weak peaks indexed as (100), (110) and (200) diffractions can be clearly observed for the samples 1 and 2, indicating the well-defined and long range ordered structure of the synthesized mesoporous materials. However, the intensity of the peaks become lower with the increase of magnesium loading, revealing the decreased regularity of the 2D hexagonal ordered structure. It is obvious that the diffraction peaks of the materials shift to higher angles with increasing magnesium loading, evidencing the magnesium has been intercalated into the walls of mesoporous silica. In addition, diffraction peaks of the used catalyst are almost the same as the newly synthesized one, manifesting the mesostructure of the catalyst is stable in the selective oxidation of cyclohexane.

The wide-angle XRD patterns are shown in figure 2. The two peaks of the typical crystalline CuO phase can be clearly observed for all samples. The curve 1 shows two diffraction peaks at about 20=35.43° and 38.67°, which could be perfectly indexed to (0 0 2) and (1 1 1) crystal faces of CuO (PDF card 45-0937, JCPDS). It is obvious that the intensity of CuO peaks decreases, moreover, the peaks get wider and smaller with increasing magnesium loading, indicating smaller CuO crystallites.²⁴ Based on the XRD data, the particle sizes of the oxides were calculated from the Scherrer equation, exhibiting average sizes of 15.3~24.7nm. Significant small amount of Cu₄MgO₅ (PDF card 47-0681, JCPDS) spinel phase can be observed on 0.6Mg-2.3Cu/SBA-15 and 1.2Mg-2.3Cu/SBA-15 samples. The peaks of MgO can not be observed in Figure. 2, most likely due to the high dispersion and low loading of this oxide over the support.^{24, 26} With the increase of magnesium, rightward shift of

the CuO diffraction peaks can also be seen as shown in Figure 2.

The N₂ adsorption-desorption analysis of the samples are shown in Figure 3. All of the samples indicate a type IV isotherm with H1 hysteresis, which is typical for mesoporous structure. The structure parameters and the amounts of the supported metals in all samples are listed in Table 1. The BET areas, pore sizes and volumes of the bi-component samples slightly decrease in comparison with the parent SBA-15 support. The contents of copper and magnesium in the final catalysts xMg-2.3Cu/SBA-15 should be in line with the theoretical ones, because the oxides were transformed directly from their corresponding inorganic salts, while the data measured by EDS were used only for reference. Some data obtained by EDS differ from the theoretical value as shown in table 1, which is presumably ascribed to the difference of the composition between the surface and bulk phase or inhomogeneous distribution of the oxides near the measuring points.

Table 1 Structure parameters of the samples and the contents of Mg and Cu measured by EDS

Sample	S(m ² /g)	Pore width (nm)	Pore volume(cm ³ /g)	Cu(wt%)	Mg(wt%)
SBA-15	525	3.8	1.08	_	
2.3Cu/SBA-15	501	4.1	1.09	3.3	
0.3Mg-2.3Cu/SBA-15	505	4.0	1.08	2.3	0.2
0.6Mg-2.3Cu/SBA-15	461	4.0	1.00	2.3	0.4
1.2Mg-2.3Cu/SBA-15	462	4.2	1.02	2.6	0.9

The TEM images of catalysts are shown in Figure 4. The well-resolved meso-channels are clearly presented for the samples 2.3Cu/SBA-15 and 1.2Mg-2.3Cu/SBA-15, which indicates that the ordered mesostructure of parent

SBA-15 was not destroyed by the introduction of copper and magnesium oxide. Little CuO particles (Fig.4) or aggregations are observed outside or inside the channel, evidencing the even dispersion of the particles, presumably owing to the lower loading of the oxides. These results are consistent with the low-angle XRD results above.

Figure 4

Figure 5

The XPS spectra of 2.3Cu/SBA-15 and 1.2Mg-2.3Cu/SBA-15 catalysts are illustrated in Figure 5. The binding energy of Cu2p_{3/2} is centered at 933.6 eV for the sample of 2.3Cu/SBA-15, the peak position (933.6eV) is in excellent agreement with that of standard CuO.^{27, 28} However, for the sample of 2.3Cu/SBA-15, the shift of Binding Energy of Cu2p_{3/2} from 933.6 to 933.2 eV can be observed, which indicated the existence of different chemical circumstances for the Cu²⁺ species and the valence state of copper species was lower.²⁹ The result could be attributed to the interaction between the copper and magnesium.

Figure 6

In figure 6, the UV-Vis absorption spectrometries of all samples are shown. There is a weak absorption peak in 244 nm for the sample 2.3Cu/SBA-15, which is due to the isolated Cu²⁺ ions and the surface oxygen.³⁰ DR UV-vis spectra of bi-component copper- and magnesium-containing SBA-15 samples show more intensive bands in about 220 nm, which is in accord with the XRD measurement in that the formation of crystalline Cu₄MgO₅ is registered. With the increase of magnesium loading, we observed that the absorption peak of plot 3 at 222 nm shifted to 221 nm (plot 4), 215 nm (plot 5) respectively, for which the Mg-O-Cu-type oxide species could be largely responsible. It may indicate that the electronic transition

energies of Mg-O-Cu-type oxide species are higher than that of Cu-O-Cu-type oxide species.

Figure 7

The H₂-TPR profiles of the samples are showed in Figure 7. These spectra exhibit narrow and nearly symmetrical main reduced peaks centered at 556 K. The 2.3Cu/SBA-15 sample shows two peaks at 544 K and 614 K, and the reduction peak at 544 K may be assigned to highly dispersed CuO and isolated Cu²⁺ ions,³¹ while the peak at 614 K could be ascribed to the reduction of black CuO particles.³² The bi-component samples only appear symmetrical single reduced peak. The higher reduction temperature peak disappeared (curve 2) when magnesium and copper were co-incorporated into Cu/SBA-15, which may be due to the improved dispersion of copper oxide.²⁴ In addition, a well-defined shift of the reduction peak from low temperature to higher temperature can also be observed for the materials xMg-2.3Cu/SBA-15 with Mg varying from 0.3 to 1.2wt%. Probably, Mg-O-Cu-type oxide species are responsible for these changes. Higher reduction temperature of the sample 1.2Mg-2.3Cu/SBA-15 compared with that of the sample 2.3Cu/SBA-15 may result from the formation of more Cu₄MgO₅. These speculations are also supported by the XRD and UV–vis data of the bi-component samples.

Table 2 Catalytic performance of different catalysts for the oxidation of cyclohexane

Catalysts	Cyclohexane Products selectivity		lectivity (mol%)	Dr. mma duata
	Conversion	Cyclohexone	Cyclohexanol(A)	By-products (%) ^a
	(mol%)	(K)		(70)
2.3Cu/SBA-15	17.4	17.8	61.4	20.8
0.3Mg-2.3Cu/SBA-15	10.5	27.6	61.2	11.2

0.6Mg-2.3Cu/SBA-15	10.7	26.6	66.3	7.1
1.2Mg-2.3Cu/SBA-15	12.0	25.7	73.6	0.7

Reaction conditions: cyclohexane 20 mL, catalyst 50 mg, temperature 423 K, oxygen 1 MPa, reaction time 70 min. ^a Byproducts mainly include adipic acid, valeric acid, formic acid cyclohexyl ester, and pentanoic acid cyclohexylesters.

The catalytic performances of different catalysts are listed in table 2. It is found that the selectivity of K/A oil are greatly improved with the bi-component samples. Specifically, the selectivity of cyclohexanone increases by nearly 10% for all bi-component catalysts, while the selectivity of cyclohexanol rises by about 10% with 1.2Mg-2.3Cu/SBA-15 as catalyst. These results indicate the addition of magnesium has a positive effect on preventing the deep oxidation of ketone for cyclohexane oxidation.

The selectivity of K/A oil increased up to 99.3% over 1.2Mg-2.3Cu/SBA-15 with conversion of cyclohexane being as high as 12%. For all we know, this is the best result for the selective oxidation of cyclohexane with molecular oxygen as oxidant.

The supposed formation pathway of CyOOH on different catalyst surface is shown in Figure 8. Owing to the low electron density of copper ion caused by the incorporation of magnesium, we inferred, the stability of intermediate 8 is much higher than that of intermediate 3 (Figure 8: a and b). Consequently, the formation rate of CyOOH released from intermediate 8 becomes slower, leading to the decrease of CyOOH in reaction system. As a result, the reaction equilibrium (equation M) shifts toward the right side. 33, 34 Thus, the consumption rate of cyclohexanone and the amount of cyclohexoxy radicals (CyO•) decrease. In addition, the lower concentration of the high-active CyO• is more easily and timely consumed by cyclohexane and O₂,

this avoids the generation of ring-opened ω-formyl radical (CHO-(CH2)4-CH2•).35

In conclusion, the high selectivity of K/A oil would be ascribed to the mild formation rate of CyO• over the catalyst 1.2Mg-2.3Cu/SBA-15.

Figure 8

The effect of the reaction temperature is illustrated in Figure 9. The conversion of cyclohexane rose with the increase of reaction temperature while the selectivity of K/A oil increased with elevating the reaction temperature from 403 K to 423 K and decreased from 423 K to 433 K. Moreover, the selectivity reached to a maximum of 99.3% at 423 K. It is well known that the reactivity of cyclohexanone and cycohexanol is higher than that of cyclohexane. The above results may result from the kinetics difference with temperature for the transformation of cyclohexane and deep oxidation of K/A oil. The selectivity of cyclohexanone also reached its maximum of 25.7% at 423K. The molar ratio of K to A reached its maximum of 0.5 at 413K and went down for the higher temperature. To get more desired products, the reaction temperature of 423 K is the most suitable for the catalyst 1.2Mg-2.3Cu/SBA-15.

Figure 9

The influence of the reaction time was investigated for the catalyst 1.2Mg-2.3Cu/SBA-15 at 423K with oxygen pressure of 1 MPa, the results are shown in Figure 10. It can be found the conversion of cyclohexane steadily increases with

reaction time. The highest selectivity of K/A oil is 99.7% at 50 min, and the selectivity of K/A oil decreases gradually with a further increase in reaction time, which is most possible due to the deep oxidation of cyclohexanol and cycloheanone. It is obvious that the excessive reaction time is unfavorable to the selectivity of K/A oil.

Figure 10

The effect of the oxygen pressure is shown in Figure 11. It indicates that the conversion of cyclohexane rises with the increase of reaction pressure. However, the selectivity of K/A oil decrease rapidly when the pressure is above 1MPa. The changing trend of the cyclohexanol is almost the same as that of K/A oil in contrast to the gentle decreasing trend of the cyclohexanone with the increase of O_2 pressure. These results may be attributed to the further oxidation of cyclohexanol to cyclohexanone as reported earlier by our group 1,2 .

Figure 11

In order to examine the stability of the catalyst 1.2Mg-2.3Cu/SBA-15, cycling experiment was conducted by reusing the catalyst in the selective oxidation of cyclohexane. The catalyst was removed from the reaction mixture by centrifugation after each reaction and washed by ethanol, followed by drying at 253 K overnight. The results of the recycle are listed in table 3, which reveal that the catalyst 1.2Mg-2.3Cu/SBA-15 still remained a good performance even after the four-time cycling, showing the good stability of this catalyst.

Cycle of catalyst **Byproduct** Cyclohexane Products selectivity (mol%) and leaching test Conversion (mol%) Cyclohexone (K) Cyclohexanol(A) (%)Trace Trace Leaching test Trace Trace 25.7 73.6 0.7 First(fresh) 12.0 Second 10.6 21.7 76.9 0.7 Third 11.7 21.8 73.6 0.6 9.3 72.1 Fourth 24.3 3.6

Table 3 The Results of Recycling and Leaching test with the Catalyst 1.2Mg-2.3Cu/SBA-15 for the cyclohexane oxidation reaction

Reaction conditions: cyclohexane 20 mL, catalyst 50 mg, temperature 423 K oxygen 1 MPa, reaction time 70 min. Byproducts mainly include adipic acid, valeric acid, formic acid cyclohexyl ester, and pentanoic acid cyclohexyl esters.

Conclusions

We have synthesized novel catalysts *x*Mg-2.3Cu/SBA-15. The newly synthesized catalysts, especially 1.2Mg-2.3Cu/SBA-15, catalyzed the selective oxidation of cyclohexane by molecular oxygen more effectively than the catalyst 2.3Cu/SBA-15. The prominent catalytic performance of the novel catalyst for the talked reaction is attributed to the incorporation of magnesium which plays a crucial role on improving the selectivity of K/A oil. Further, catalysts *x*Mg-2.3Cu/SBA-15 bear a promoted dispersion of the active components, the incorporated magnesium can prevent the deep oxidation of the goal products, most likely due to the weak electronic transition of the Mg-O-Cu-type oxide species.

The best catalytic results, in terms of highest selectivity of K/A oil and a good conversion of cyclohexane, were obtained with the catalyst 1.2Mg-2.3Cu/SBA-15. The catalyst xMg-2.3Cu/SBA-15 can serve as a promising candidate catalyst for industrial application, and are worth studying intensively for the mentioned reaction.

Experimental

Syntheses

SBA-15. The mesoporous molecular sieves SBA-15 were prepared according to the hydrothermal method delineated by Stucky et al.³⁶ 4 g of P123 (Aldrich, EO₂₀PO₇₀EO₂₀, M = 5800) was dissolved in 20 g of deionized water and 80 g of a 2 M HCl solution under stirring at 313 K, then Tetraethyl orthosilicate (TEOS) was slowly added. After stirring at 313 K for 24 h, the mixture was transferred to a Teflon-lined stainless steel autoclave to undergo a static hydrothermal treatment at 393 K for 48 h. The solid products were filtered off, washed with deionized water until no Cl⁻ was detected using AgNO₃ solution, and dried at 353 K overnight. The samples obtained were calcined in air at 823 K for 6 h to remove the template.

Magnesium-Copper-supported SBA-15. The metal-containing SBA-15 mesoporous materials were prepared at room temperature by impregnation method. The mesoporous SBA-15 material was impregnated with an ethanol solution of copper(II) nitrate trihydrate and magnesium nitrate hexahyrate in stoichiometric proportion, keeping stirring for 10h. Then the synthesized samples were dried at 373 K for 12 h, and followed by calcination at 623 K for 3 h. The metal-containing materials were labeled as 2.3Cu/SBA-15 (the number before the element denotes its theoretical percentage by mass in the catalyst, hereafter inclusive), 0.3Mg-2.3Cu/SBA-15, 0.6Mg-2.3Cu/SBA-15 and 1.2Mg-2.3Cu/SBA-15.

Catalyst Characterization

X-Ray powder diffraction (XRD) patterns were recorded on a XRD-6000 (Shimadzu, Japan) system with a Cu-K α radiation of wavelength =0.15418 nm (40 kV,

40mA). The solid ultraviolet-visible (UV-vis) spectra were measured on a UV-VIS-NIR (UV-visible Near Infra-Red) scanning spectrophotometer (Shimadzu, UV-3600 PC) with an ISR-3100 integrating sphere attachment and BaSO₄ as an internal reference. N₂ adsorption-desorption isotherms were measured at 77 K on an volumetric automatic sorption analyzer (Micromeritics, ASAP2020). Temperature-programmed reduction of hydrogen (H₂-TPR) was performed by using a homemade apparatus loaded with 20 mg of sample. The samples were pretreated at 573 K for 1 h and then cooled to 303 K under a N₂ flow. A gas mixture consisting of 10% H₂ in argon was injected until adsorption saturation was reached, followed by a flow of N₂ for 30 min. Then the temperature was raised from 303 K to 873 K at a heating rate of 10 k/min, and the amount of desorbed hydrogen was measured by a thermal conductivity detector (TCD). The copper and magnesium contents in the catalysts were determined by scanning electron microscope and Energy Dispersive Spectrometer (SEM-EDS) (S-3400N, X Flash Detector 4010). Transmission electron microscopy (TEM) was conducted on a JEM 2100F electron microscope operated at 200 kV. X-ray photoelectron spectroscopy (XPS) signals were collected on a PHI-5000C ESCA system (Perkin Elmer) with Al K α radiation (hv = 1486.6 eV) Calibration of the binding energies was made with the C1s binding energy of standard hydrocarbons (284.6 eV).

Catalytic Property Testing

Selective oxidation of cyclohexane was carried out in a 100 mL Teflon-lined

stainless-steel autoclave equipped with a magnetic stirrer. Typically, 20 mL of cyclohexane and 50 mg of solid catalyst were added into the reactor. The reaction was conducted under the conditions of 403 K~433 K and a pressure of 0.6 Mpa~2.4 MPa controlled by O₂ with a stirring rate of 800 rpm. During the oxidation process, the O₂ pressure was kept between 0.8 MPa and 1 MPa. After a predetermined time of reaction, the reactor was cooled to room temperature with cool water, and centrifuged to separate the catalyst. An excessive amount of triphenylphosphine (Ph₃P) was added to the reaction mixture to completely reduce the cyclohexylhydroperoxide (CHHP), an intermediate in the cyclohexane oxidation to cyclohexanol. The products were analyzed using a gas chromatograph (FULI 9790 series GC,AE.PEG-20M, FID, CHINA) equipped with a capillary column (30 m long, 0.32 mm i.d., 0.5 um film thickness) and a FID detector using toluene as the internal standard. The conversion was calculated based on the starting cyclohexane.

Leaching and recycling tests

In order to identify whether the cyclohexane oxidation is due to the catalytic effect of Cu²⁺, a leaching test was carried. Typically, 20 mL of cyclohexane and 50 mg of solid catalyst were added into a 100 mL reactor. The reaction was conducted under the condition of 423 K and 1 MPa pressure controlled by N₂ with a stirring rate of 800 rpm. After a predetermined time of reaction, the mixture was cooled to room temperature with cool water and the catalyst was separated by centrifugation. The solution was then charged with O₂ under a condition as mentioned above.

The solid catalyst was recovered from the reaction mixture by separating,

washed with ethanol several times, and finally dried at 353 K for 10 h. The recovered catalysts were reused for three times under the same reaction conditions.

Acknowledgments

The authors acknowledge Shanghai Institute of Technology for the kind support in catalyst characterization and experiments.

Notes and reference

- 1 J. Li, Y. Shi, L. Xu, G. Lu, Ind. Eng. Chem. Res., 2010, 49, 5392-5399.
- 2 R. Zhao, Y. Wang, Y. Guo, Green. Chem., 2006, 8, 459-466.
- 3 J. Li, L. Xu, Y. Shi, Catal. Lett., 2010, 137, 180–189.
- 4 H. Zhao, J. Zhou, H. Luo, C. Zeng, D. Li, Y. Liu, Catal. Lett., 2006, 108, 49-54.
- 5 P. Wu, Z. Xiong, K. P. Loh, X. S. Zhao, Catal. Sci. Technol., 2011, 1, 285-294.
- 6 J. Gu, Y. Huang, S. P. Elangovan, Y. Li, W. Zhao, I. Toshio, Y. Yamazaki, J. Shi, J. Phys. Chem. C, 2011, 115, 21211-21217.
- 7 J. S. Reddy, S. Sivasanker, Catal. lett., 1991, 11, 241-244.
- 8 S. Shylesh, Ch. Srilakshmi, A. P. Singh, B. G. Anderson, Micropor. Mesopor. Mater., 2007, 99, 334-344.
- 9 S. Samanta, N. K. Mal, A. Bhaumik, J. Mol. Catal. A: Chem, 2005, 236, 7-11.
- 10 S. E. Dapurkar, A. Sakthivel, P. Selvam, New J. Chem., 2003, 27, 1184-1190.
- 11 P. Wu, P. Bai, Z. Lei, K. P. Loh, X. S. Zhao, Micropor. Mesopor. Mater., 2011, 141, 222-230.
- 12 N. Yu, Y. Ding, A. Y. Lo, S. J. Huang, P. H. Wu, C. Liu, D. Yin, Z. Fu, D. Yin, C. T. Hung, Z. Lei, S. B. Liu, Micropor. Mesopor. Mater., 2011, 143,426-434.
- 13 L. Chen, J. Hu, R. Richards, J. Am. Chem. Soc., 2009, 131, 914-915.
- 14 R. Zhao, D. Ji, G. Lv, G. Qian, L. Yan, X. Wang, J. Suo, Chem. Commun., 2004, 7, 904-905.
- 15 G. Lü, D. Ji, G. Qian, Y. Qi, X. Wang, J. Suo, Appl. Catal. A: Gen, 2005, 280,

- 175-180.
- 16 K. Zhu, J. Hu, R. Richards, Catal. Lett., 2005, 100, 195-199.
- 17 B. K. Min, C. M. Friend, Chem. Rev., 2007, 107, 2709-2724.
- 18 L. F. Gutiérrez, S. Hamoudi, K. Belkacemi, Catal. Rev., 2011, 1, 97-154.
- 19 P. Haack, C. Limberg, K. Ray, B. Braun, U. Kuhlmann, P. Hildebrandt, C. Herwig, Inorg. Chem., 2011, 50, 2133-2142.
- 20 O. P. H. Vaughan, G. Kyriakou, N. Macleod, M. Tikhov, R. M. Lambert, J. Catal., 2005, 236, 401-404.
- 21 K. Machado, S. Mukhopadhyay, G. S. Mishra, J. Mol. Catal. A: Chem, 2015, 400, 139-146.
- 22 H. Yoshida, T. Tanaka, M. Yamamoto, T. Funabiki, S. Yoshida, Chem. Commun., 1996, 18, 2125-2126.
- 23 H. Zhang, M. Li, P. Xiao, D. Liu, C. J. Zou, Chem. Eng. Technol., 2013, 36, 1701-1707.
- 24 A. J. Vizcaíno, A. Carrero, J. A. Calles, Catal. Today., 2009, 146, 63-70.
- 25 A. Metzger, S. Bernhardt, G. Manolikakes, P. Knochel, Angew. Chem. Int. Ed., 2010, 49, 4665-4668.
- 26 A. Carrero, J. A. Calles, A. J. Vizcaíno, Appl. Catal. A: Gen, 2007, 327, 82-94.
- 27 Y. Okamoto, K. Fukino, T. Imanaka, S. Teranishi, J. Phys. Chem. 1983, 87, 3740-3747.
- 28 B. Peplinski, W. Unger, I. Grohmann, Appl. Surf. Sci. 1992, 62, 115-129
- 29 W. L. Dai, Q. Sun, J. F. Deng, D. Wu, Y. H. Sun, Appl. Surf. Sci. 2001, 177, 172-179.
- 30 M. C. Marion, E. Garboeski, M. Primet, J. Chem. Soc. Faraday. Trans., 1990, 86, 3027-3032.
- 31 X. Lu, Y. Yuan, Appl. Catal. A: Gen, 2009, 365, 180-186.
- 32 C. H. Tu, A. Q. Wang, M. Y. Zheng, X. D. Wang, T. Zhang, Appl. Catal. A: Gen, 2006, 297, 40-47.
- 33 I. Hermans, P. A. Jacobs, J. Peeters, J. Mol. Catal. A: Chem, 2006, 251, 221-228.
- 34 I. Hermans, P. A. Jacobs, J. Peeters, Chem. Eur. J., 2006, 12, 4229-4240.

35 J. D. Druliner, P. J. Krusic, G. F. Lehr, C. A. Tolman, J. Org. Chem., 1985, 50, 5838-5845.

36 D. Zhao, J. Feng, Q. Huo, N. Melosh, G. H. Fredrickson, B. F. Chmelka, G. D. Stucky, J. Am. Chem. Soc. , 1998, 120, 6024-6036.

- Figure 1.Small angle XRD patterns of all samples
- Figure 2. Wide angle XRD patterns of all samples
- **Figure 3.**N₂ adsorption-desorption isotherms of the samples.
- Figure 4.TEM images of catalysts (a) and (c) 2.3Cu/SBA-15, (b) and (d) 1.2Mg-2.3Cu/SBA-15.
- Figure 5. XPS spectra of Cu 2p of samples 2.3Cu/SBA-15 and 1.2Mg-2.3Cu/SBA-15
- Figure 6. UV-Vis absorption spectra for the samples
- Figure 7. H₂-TPR profiles of the samples.
- **Figure 8.** a) Propagation reactions in the formation of CyOOH on the catalyst 2.3Cu/SBA-15. b) Propagation reactions in the autoxidation of cyclohexane for the catalyst 1.2Mg-2.3Cu/SBA-15.
- **Figure 9.** Relationship between temperature and reaction results over 1.2Mg-2.3Cu/SBA-15. Reaction conditions: cyclohexane 20 mL, catalyst 50 mg, oxygen 1 MPa, reaction time 70 min.
- **Figure 10.** Dependence of the conversion and selectivity on reaction time in cyclohexane oxidation over the catalyst 1.2Mg-2.3Cu/SBA-15. Reaction conditions: cyclohexane 20 mL, catalyst 50 mg, oxygen 1 MPa, reaction temperature 423 K.
- **Figure 11.** Relationship between pressure and reaction results over 1.2Mg-2.3Cu/SBA-15. Reaction conditions: cyclohexane 20 mL, catalyst 50 mg, reaction time 70 min, reaction temperature 423 K.

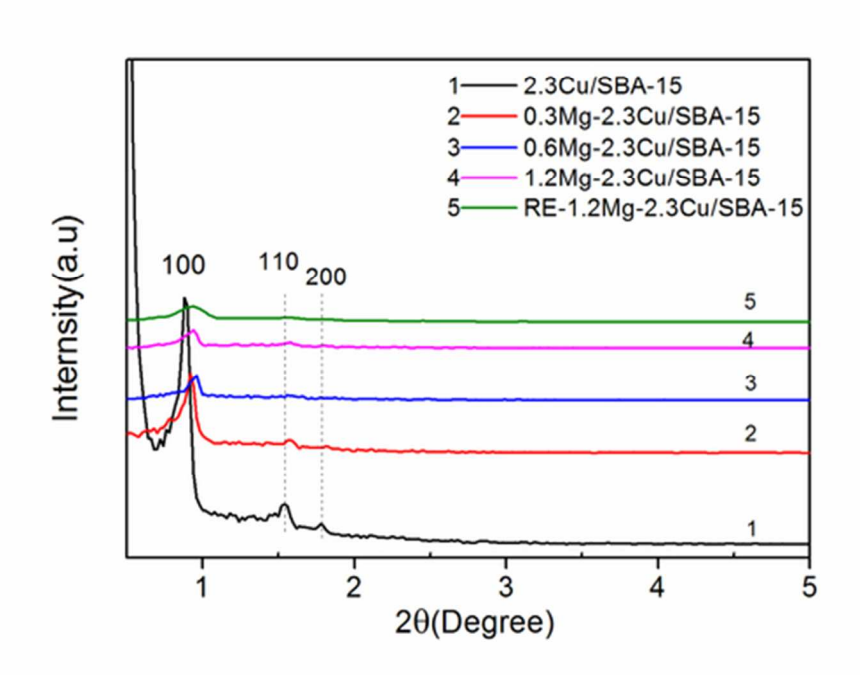


Figure 1. Small angle XRD patterns of all samples 48x33mm (300 x 300 DPI)

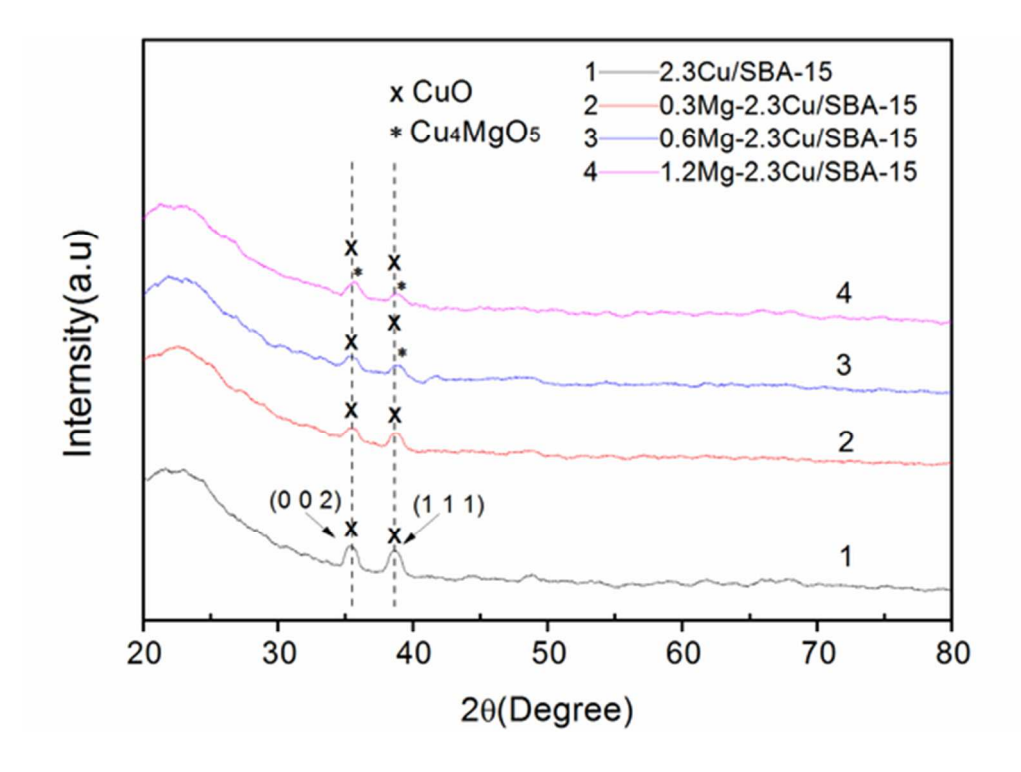


Figure 2.Wide angle XRD patterns of all samples 48x33mm (300 x 300 DPI)

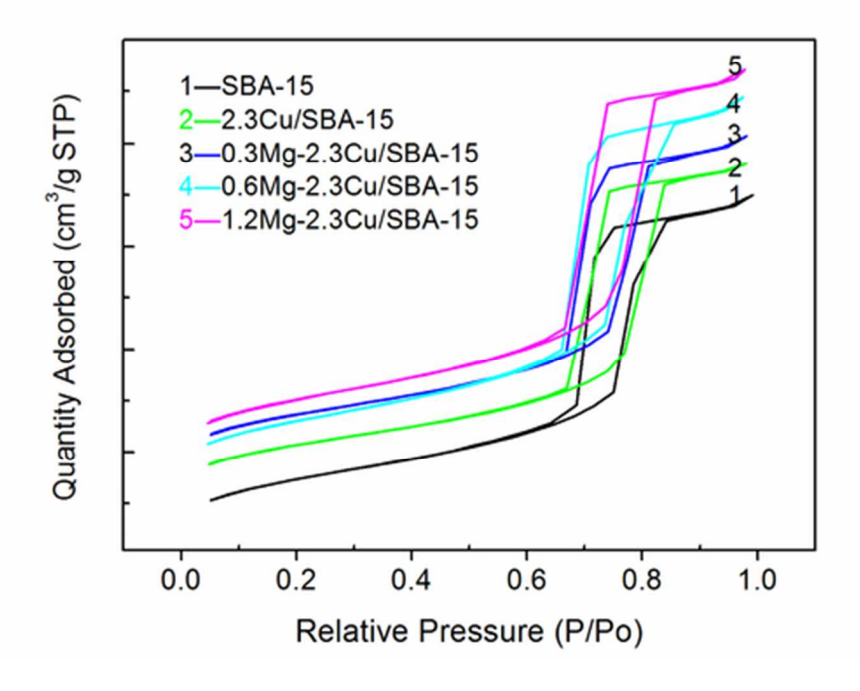


Figure 3.N2 adsorption-desorption isotherms of the samples. 48x33mm (300 x 300 DPI)

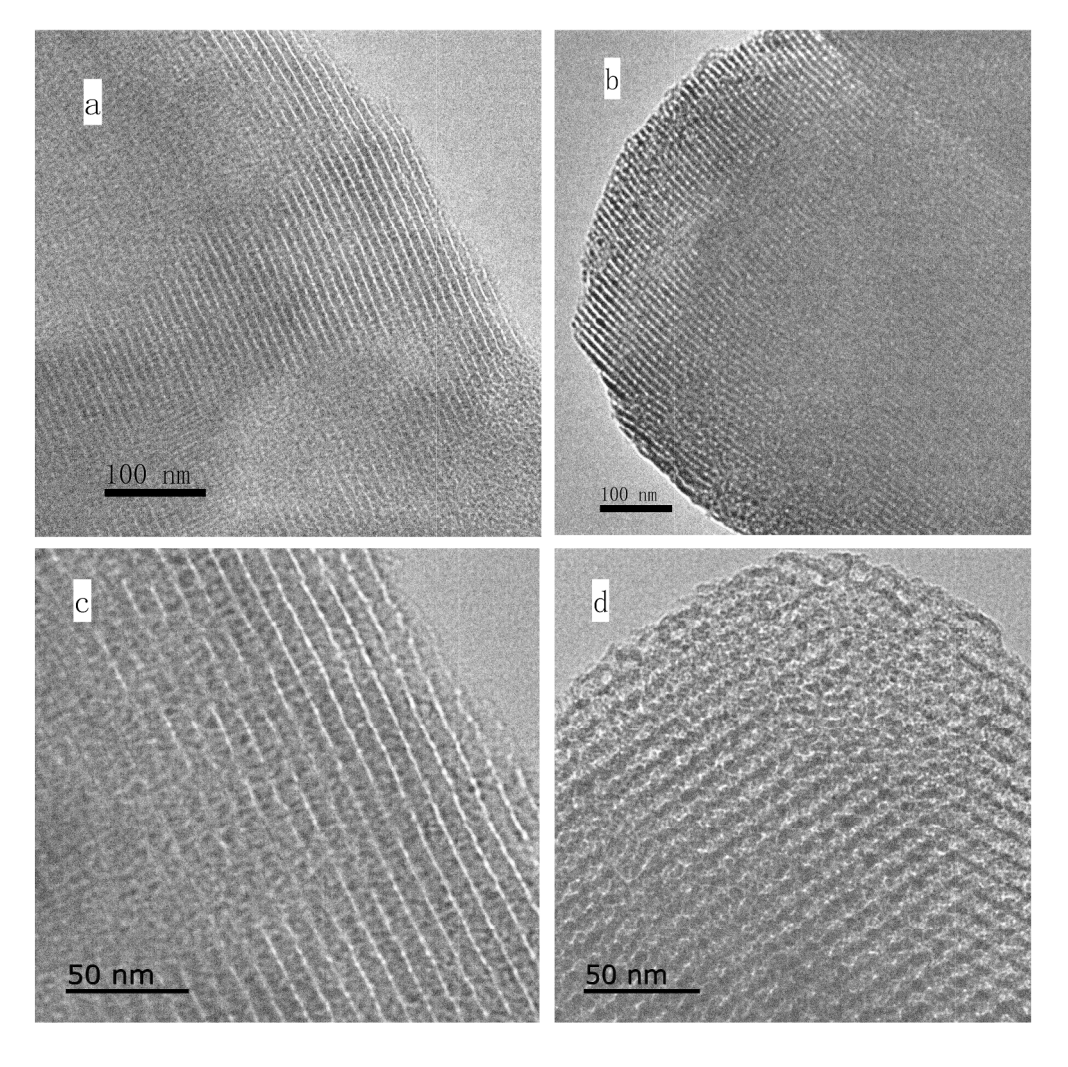


Figure 4.TEM images of catalysts (a) and (c) 2.3Cu/SBA-15, (b) and (d) 1.2Mg-2.3Cu/SBA-15.

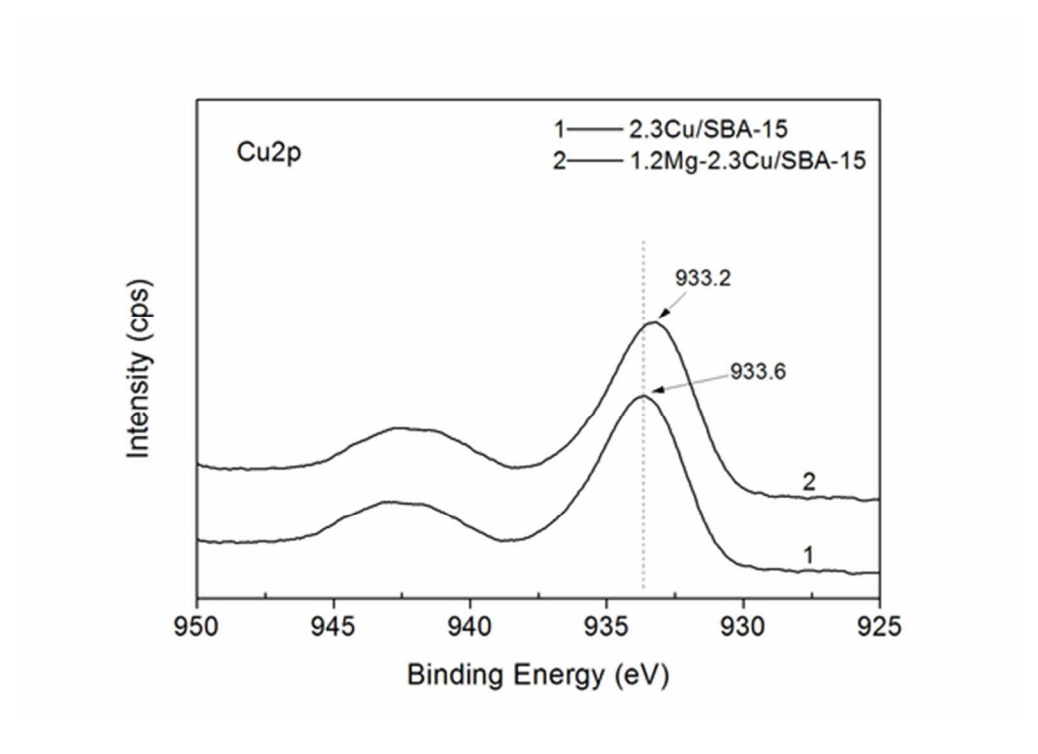


Figure 5. XPS spectra of Cu 2p of samples 2.3Cu/SBA-15 and 1.2Mg-2.3Cu/SBA-15 $\,$ 48x33mm (300 x 300 DPI)

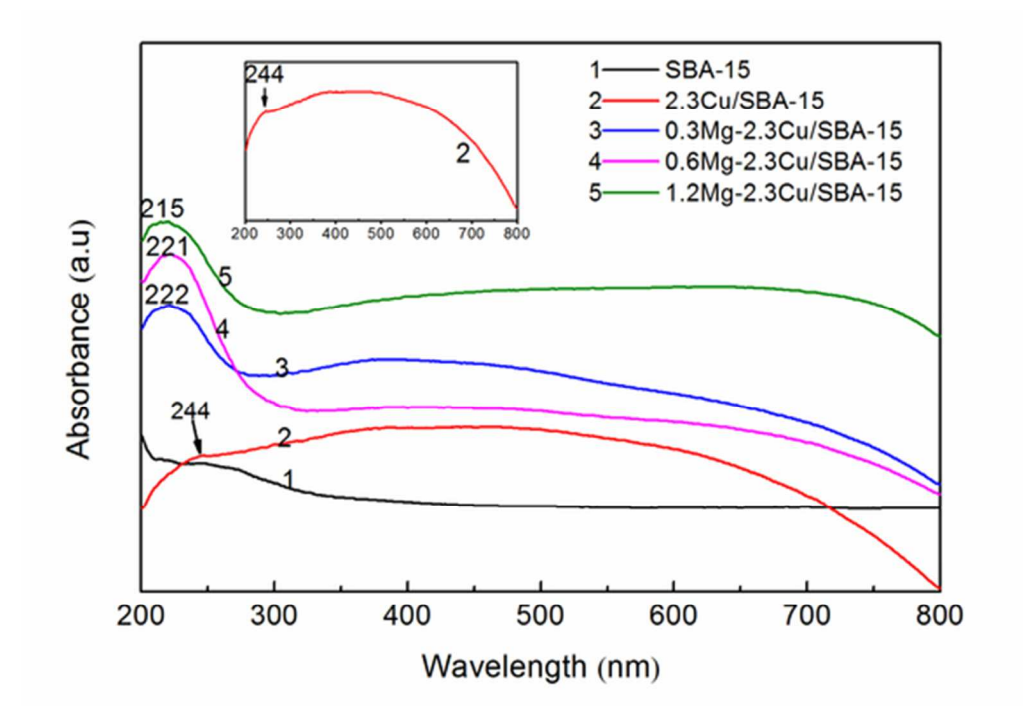


Figure 6. UV-Vis absorption spectra for the samples $48x33mm (300 \times 300 DPI)$

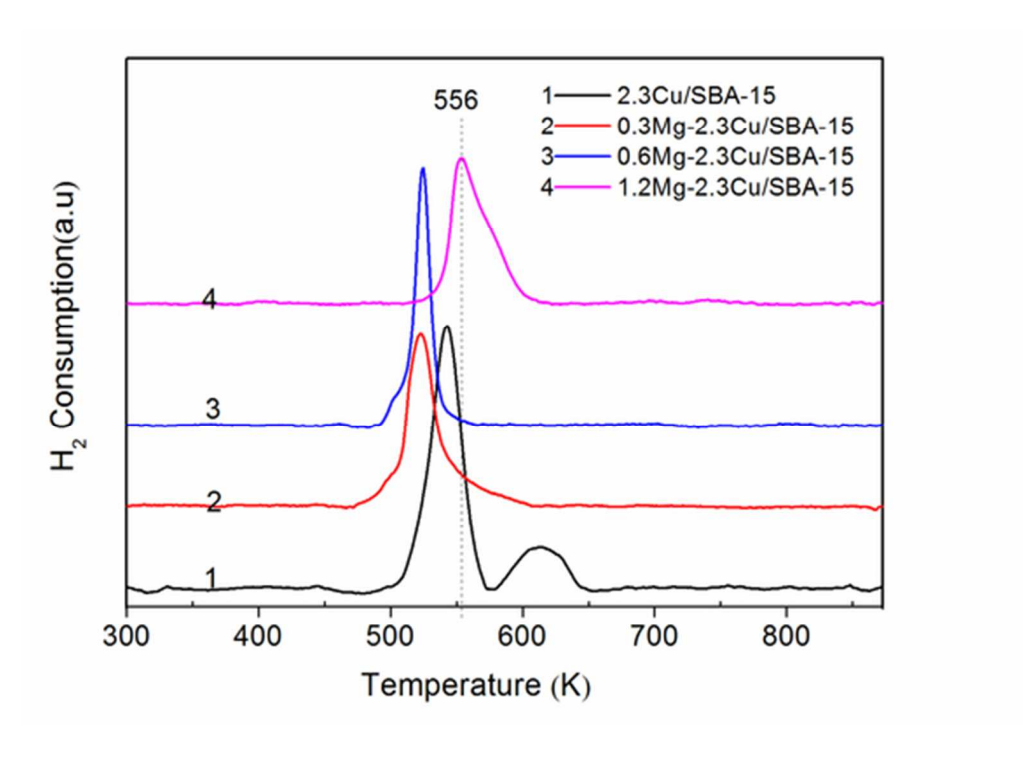


Figure 7. H2-TPR profiles of the samples. 48x33mm (300 x 300 DPI)

Figure 8. a) Propagation reactions in the formation of CyOOH on the catalyst 2.3Cu/SBA-15 80x39mm~(300~x~300~DPI)

Figure 8. b) Propagation reactions in the autoxidation of cyclohexane for the catalyst 1.2Mg-2.3Cu/SBA-15 158x141mm (300 x 300 DPI)

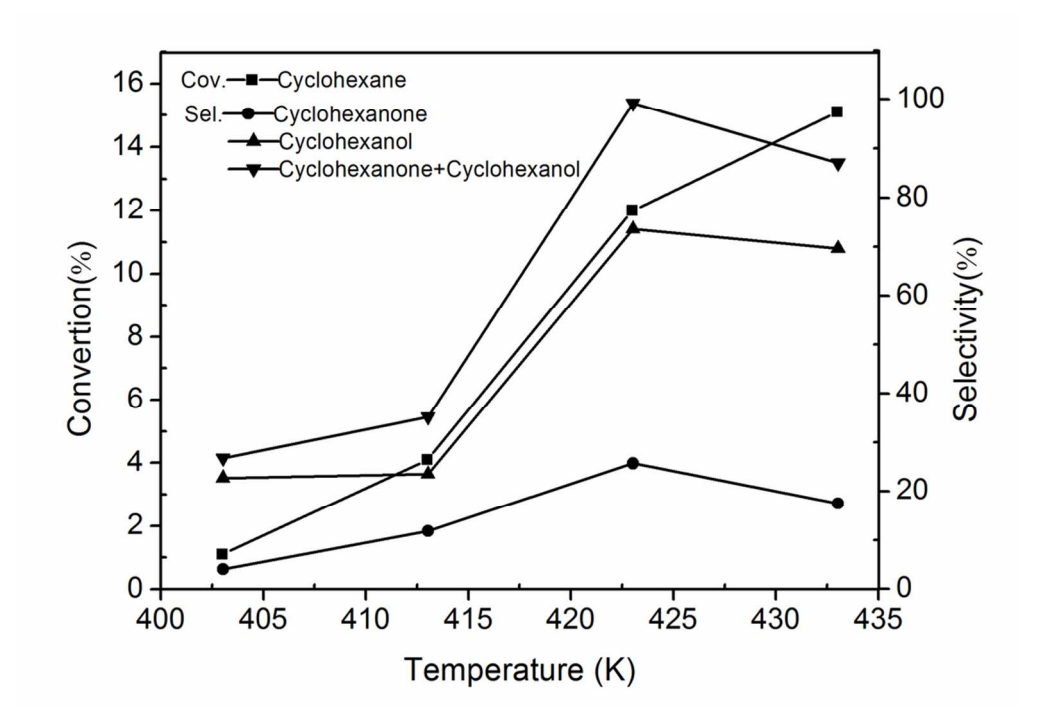


Fig.9 Relationship between temperature and reaction results over 1.2Mg-2.3Cu/SBA-15. Reaction conditions: cyclohexane 20 mL, catalyst 50 mg, oxygen 1 MPa, reaction time 70 min 48x33mm (600 x 600 DPI)

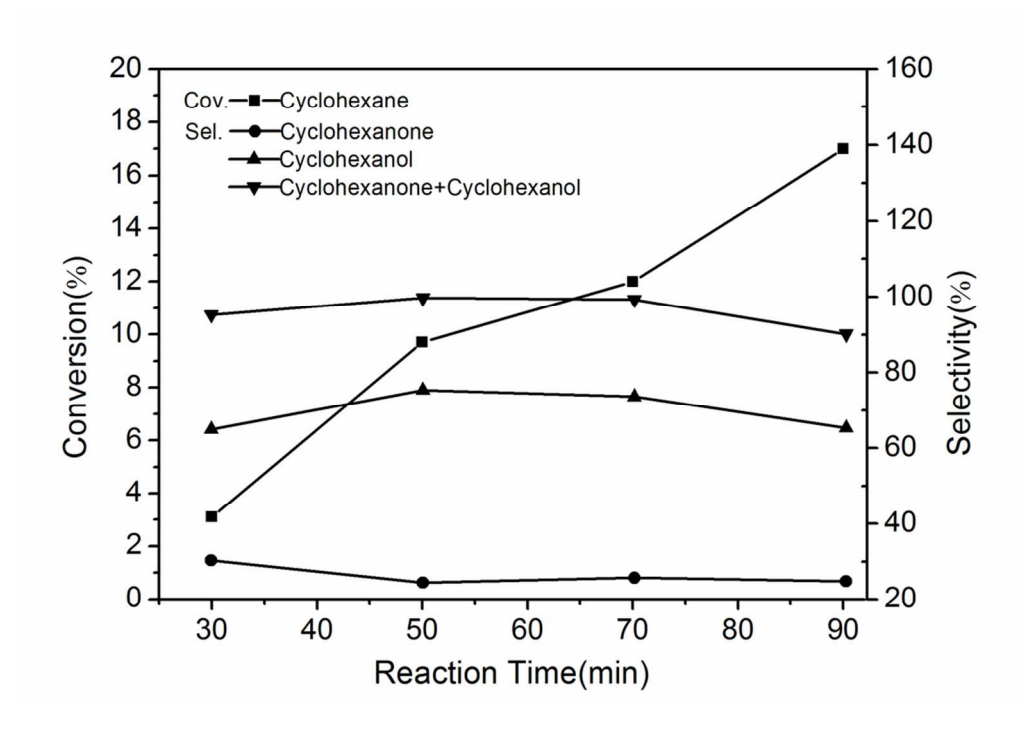


Fig.10 Dependence of the conversion and selectivity on reaction time in cyclohexane oxidation over the catalyst 1.2Mg-2.3Cu/SBA-15. Reaction conditions: cyclohexane 20 mL, catalyst 50 mg, oxygen 1 MPa, reaction temperature 423 K
48x33mm (600 x 600 DPI)

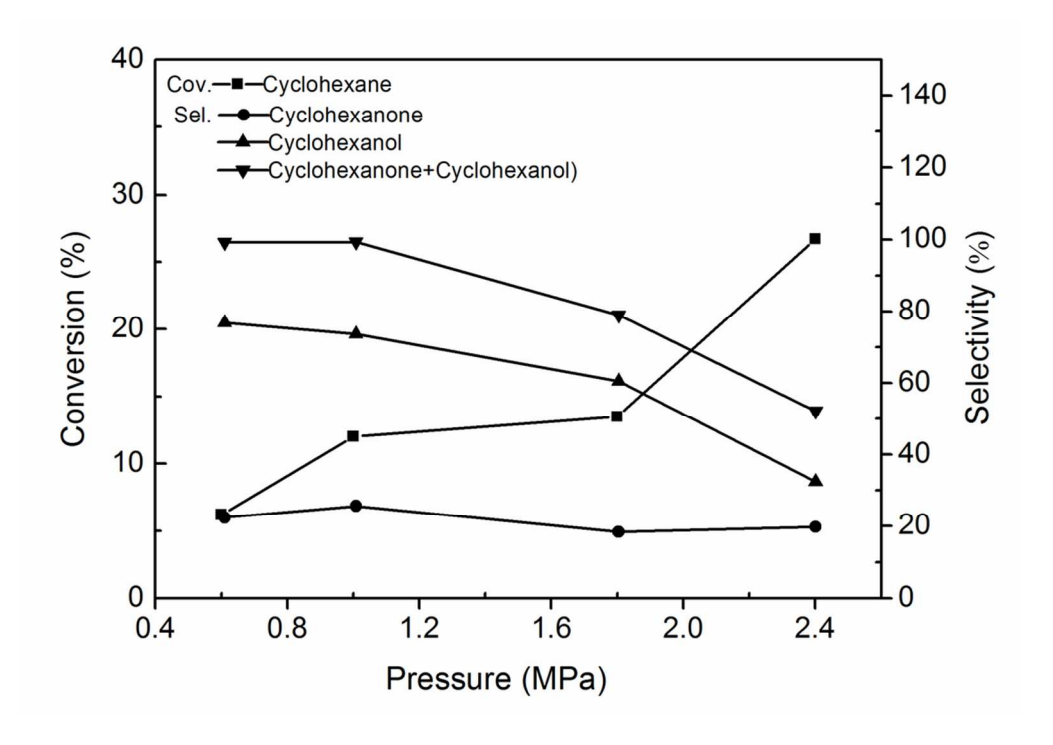


Fig.11 Relationship between pressure and reaction results over 1.2Mg-2.3Cu/SBA-15. Reaction conditions: cyclohexane 20 mL, catalyst 50 mg, reaction time 70 min, reaction temperature 423 K $48 \times 33 \text{mm}$ (600 x 600 DPI)

Novel catalysts by co-supporting copper and magnesium oxide on mesoporous silica exhibited a special catalytic activity and selectivity for the liquid-phase oxidation of cyclohexane by O2 158x141mm (300 x 300 DPI)